# Hydrodynamic Assessment of Double-Ended Ferry for Operation in Venice

Enrico DELLA VALENTINA[a], Victor FERRARI[a,1]
Andrea BORTOLATO[b], Antonio FERRARI[c]
[a] *MARIN – Maritime Research Institute Netherlands*
[b] *inNave S.r.L.* [c] *ACTV S.p.A.*

**Abstract.** The present paper discusses a practical case study of a hydrodynamic assessment for a double-ended ferry designed to operate in the Venice's lagoon. The main objective of this study was to compare two propulsive configurations, with 2 or with 4 azimuthing thrusters, both in terms of powering and manoeuvrability performances. Additional design requirements were: good ship handling, even in case of one propulsor failure, and a limited drift angle. The results of this overall hydrodynamic assessment gave important indications on the performance of the ship and helped the definition of the optimal ship design.

**Keywords.** Powering, manoeuvring, model tests, CFD, simulations, double-ended ferry

## 1. Introduction

In 2020, Venice's public transport company ACTV S.p.A., the design office inNave S.r.L. and the Maritime Research Institute Netherlands (MARIN) collaborated for a hydrodynamic assessment of ACTV's next generation vessel. The concept vessel is a 55 m double-ended RoPax ferry due to operate in the lagoon of Venice. An artist's impression is shown in Figure 1 and its main particulars in Table 1. However, the hydrodynamic assessment of double-ended ferries is always particularly challenging [1], not only due to their peculiar hull shape, but also because of the environment where they have to operate and its related constraints. In this particular case, two configurations had to be tested and compared: one consisting of two azimuth thrusters fitted one at each end of the ship, and the second with four azimuth thrusters, of which two are installed at each end. The design requirement were: hull and propulsion optimized not only for low resistance in deep and shallow water, at high and low speeds, but also good manoeuvrability including in emergency situations. These requirements derive from the fact that the ship has to safely operate in the busy, narrow and shallow Venetian canals, sometimes even in presence of debris floating around or poor visibility due to fog. These constraints found in Venice require special attention and dedicated approaches [2].

The first step of the assessment was a hull optimisation by means of RANS calculations, taking into account the required adjustments in the hull between the two configurations. Successively, resistance and propulsion model tests highlighted the

[1] Corresponding author. Address: MARIN, Haagsteeg 2, 6708PM, Wageningen, the Netherlands. E-mail: v.ferrari@marin.nl.

differences in powering performance between the two configurations. The tests also showed the optimal power distribution between fore and aft propulsion for both configurations.

The manoeuvring assessment also consisted in both experimental and numerical parts. First model tests were carried out for evaluating the low speed manoeuvrability of both configurations, including the case of one propulsor failure. Then the experimental results were used to tune a numerical model, which was used to perform a broader range of manoeuvres such as at high speeds or small helm angles.

In the end the results of this overall hydrodynamic assessment gave important indications on the performance of the ship and helped the definition of the optimal ship design.

**Figure 1.** Artist's impression of the next generation ACTV ferry.

**Table 1.** Main particulars at design draught and propeller characteristics of the 4 thruster (4T) and 2 thruster (2T) configurations.

| Particular | Symbol | Value 4T | Value 2T |
|---|---|---|---|
| Length between perpendiculars | $L_{PP}$ | 55.000 | |
| Breadth moulded on WL | B | 12.994 | |
| Draught moulded on FP | $T_F$ | 2.485 | |
| Draught moulded on AP | $T_A$ | 2.458 | |
| Volume moulded | $\nabla$ | 1004.0 | |
| Block coefficient | $C_B$ | 0.568 | |
| Propeller diameter | D | 1.148 | 1.450 |
| Propeller pitch ratio at 0.7R | $P_{0.7}/D$ | 1.130 | 1.155 |
| Expanded blade area ratio | $A_E/A_0$ | 0.562 | 0.708 |
| Number of blades | Z | 4 | 4 |

## 2. Resistance and powering assessment

### *2.1. Hull optimization with RANS calculations*

The scope of the RANS computations was to investigate a possible resistance reduction by geometrical variations of the hull for one displacement and two velocities: 6 and 11 knots. In order to do so, full scale viscous flow calculations were carried out for all the geometries. At each iteration, the results of the computations were the total resistance, the dynamic trim and sinkage, the nominal wake field and all information on the flow deriving from RANS calculations, such as pressure and friction distribution, free surface elevation, reversed flow and vorticity.

For all the calculations, use has been made of the in-house developed RANS code ReFRESCO [3]. Only half a ship was modelled and the domain size was $6L_{PP}$ x $2L_{PP}$ x $3L_{PP}$ in length, width and depth, respectively, chosen to minimise the influence of boundaries on the flow solution around the vessel. Grid settings and grid density were based on best practice guidelines following from MARIN grid sensitivity studies. In particular, the number of cells depended on the hull lines and speed, ranging from 2 to 4 million cells, and the average $y^+$ value was 200. The propeller suction effect was simulated with actuator disc.

Three geometrical variations were investigated. The improvements to the hull can be summarised as:

1. Reduction of the waterline entry angle of the stern and bow below the ramps. Originally the hull presented a flat surface perpendicular to the incoming flow at the extremities. By streamlining the extremities the pressure resistance decreases.
2. Increase of the propeller - hull clearance in order to let the propellers operate in a more uniform wake and reduce the interactions with the hull.

The final hull geometry has a lower total resistance than the original hull form for both investigated velocities. The resistance reduction is about 6% at 6 knots and 7% at 11 knots. These gains come from a significant reduction of the pressure distribution at the bow, and a decrease of friction at the bilge and aft skeg.

When comparing the two optimised configurations (Figure 2), the two propellers version generates a higher pressure area in front of the fore skeg, but the four propellers configuration has a higher frictional resistance. The CFD calculations also allow to look into the wake field. Based on a qualitative assessment, the nominal wake field at the stern can be classified as good for the 2 thruster configuration and as acceptable for the 4 thruster one. For these reasons, the two propellers configuration appears to be more efficient from a resistance and powering point of view.

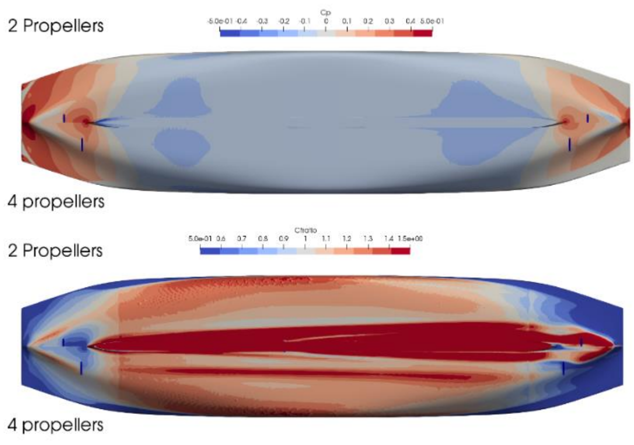


**Figure 2.** Comparison of the pressure (above) and friction distribution (below) at 11 kn between the configuration with two and four propellers (ferry sailing to the right).

### *2.2. Resistance and powering model tests*

The resistance and propulsion tests have been conducted in MARIN's Deep Water Towing Tank (DT), which measures 250 m by 10.5 m by 5.5 m in length, width and depth respectively. A view of the tank is shown in Figure 3.


**Figure 3.** MARIN's Deep Water Towing Tank.

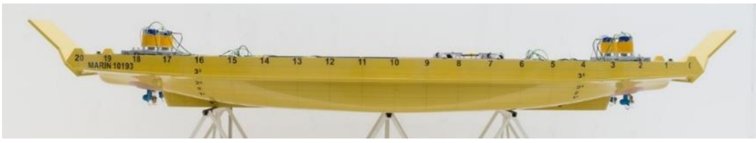

**Figure 4.** MARIN ship model No. 10193, configuration with four thrusters.

One ship model was manufactured in wood including the fore and aft ramps (Figure 4). It was prepared in such a way as to easily switch between the two configurations, by adding or removing the thrusters and headboxes, and closing the gaps in the hull where needed. Turbulence of the flow over the hull was induced by studs near the bow and by strips with carborundum at the leading edge of each appendices. The propellers in the four thrusters configuration were rotating inward over the top, whereas in the two thrusters configuration the aft propeller rotated clockwise and the fore propellers anti-clockwise. Two loading conditions were tested: design draught (draught amidship 2.472 m) and light load (draught amidship 1.751 m).

Many inputs were varied and several configurations were tested during the powering experiments, including finding the optimum thruster angle, checking the influence of the appendages and loading conditions, finding the best fore/aft power distribution. Here a brief summary of the most relevant results is presented.

Two ramp configuration were tested. In the first version the ramps touched the water at high speeds and significantly increased the resistance. Successively the ramps have been adjusted at a better position for the later propulsion tests. This hull variation showed the importance of a correct installation of the ramps with respect to the waterline and the car deck.

The increase of power due to increased displacement from light load to design load varies from about 15% at the lower speeds to about 28% at the higher speeds. The increase of power between the four and two thrusters spans from about 6% at the higher speeds to about 11% at the lower speeds.

The optimal power distribution in the four thrusters configuration is 20% on the fore and 80% on the aft thrusters. In the two thrusters configuration the optimal power distribution is 15/85. This values appear to be in line with other studies [4]. However, these power distributions would require a too high power on the aft thrusters and, as a consequence, the chosen distribution is of 30/70 for both configurations.

Finally, an important requirement for the double-ended ferry under investigation is the operation in shallow water of h = 15 m. The draught to water-depth ratio T/h and the

Froude Number water-depth V/(g·h)½, indicate that the vessel has only a minimum shallow water effect at the top speed for the full load draught with a speed loss of about 0.01 knots. It must be noted that in shallower water the losses shall be larger, but for the required water depth of 15 m the losses are very limited. Moreover, at the light load draught, the vessel does not require any shallow water correction when operating in a water depth of 15 m.

All the previous results are summarised in Figure 5 and Table 2. The latter shows the ship speeds and propeller rotation rates expected on full scale trials for the ship. The prediction is based on the powering model tests as tested, with the model equipped with all appendages and stock propulsors, in water of 15 degrees Celsius and no effects of wind nor waves.

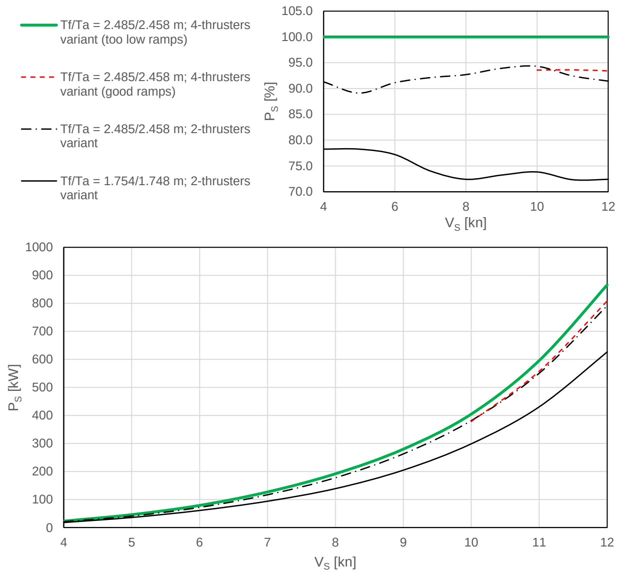


**Figure 5.** Summary of powering test results.

**Table 2.** Trial speed and propulsion rates with a total shaft power of 1000 kW in all configurations.

| Draught Fore/Aft [m] | Configuration (no. of thrusters) | Power distribution [%] | | Trial speed [kn] | |
|---|---|---|---|---|---|
| | | Fore | Aft | Deep water | Water-depth 15.0 m** |
| 2.485/2.458 | 4 | 30 | 70 | 12.39 | 12.38 |
| 2.485/2.458 | 4 | 30 | 70 | 12.58* | 12.57 |
| 2.485/2.458 | 2 | 20 | 80 | 12.67 | 12.66 |
| 2.485/2.458 | 2 | 30 | 70 | 12.64 | 12.63 |
| 1.754/1.748 | 2 | 15 | 85 | 13.20 | 13.20 |
| 1.754/1.748 | 2 | 30 | 70 | 13.14 | 13.14 |

* With optimised ramps
** Speeds estimated by semi-empirical corrections

## 3. Manoeuvring assessment

### *3.1. Free running model tests*

The manoeuvring tests were performed with the same model used in the powering experiments. The aft thrusters, 1 or 2 depending on the configuration, were steerable and used to control the vessel. The fore thrusters were not steerable and were used for propulsion only, as would happen in reality during normal operations.

The tests were performed in the Seakeeping and Manoeuvring Basin (SMB) of MARIN, shown in Figure 6. The basin measures 170 x 40 x 5 m in length, width and depth respectively. A main carriage and a sub-carriage follow the free-running model, providing the required power and collecting the measured data.

**Figure 6.** MARINS's Seakeeping and Manoeuvring Basin.

All tests were conducted with a self-propelled, free-running model. All runs were performed with constant RPM. It is considered that this did not influence the manoeuvre since the approach speed of all tests was 6 kn, which is approximatively half the maximum speed and thus is far from the maximum power limit.

In most cases the thruster steering rate was 12°/s, although some runs were performed with a lower value to investigate its impact on the manoeuvring characteristics. The manoeuvres performed consisted in zig-zags 5°/1°, 10°/10°, 20°/20°, in addition to turning circles with 35°, 25° and 20° rudder angles. These turning circles were followed by a pull-out at different rudder angles, in order to derive the instability loop of the vessel. The configuration tested were with 4 thrusters and a power distribution 30 % fore 70% aft, 2 thrusters with power distribution 30/70, 2 thrusters with 20/80 and finally, for the zig-zags 20°/20° only, also a configuration where only the aft propulsors are active, representing an emergency situation of partial propulsion failure. A selection of these results are discussed in the following paragraphs.

The overshoot angles obtained from the zig-zag runs are reported as bar diagrams in Figure 7, for the configurations 4 thruster and 2 thruster with 30/70 power balance. The graphs show how the configuration with 2 thrusters has higher overshoot angles with respect to the case 4 thrusters. Also the asymmetry between results from starboard and port side increases. This is due to the fact that the transverse force generated by the propeller rotation is not compensated when there is only one thruster per side. Moreover, as mentioned previously, the zig-zag 20°/20° manoeuvres were repeated also testing an emergency situation in which the fore thrusters would be out of service. A comparison of the overshoot and drift angles between normal and emergency operation is reported in the same figure, for the configurations 4 thrusters and 2 thrusters with 30/70 power balance. It can be seen how stopping the fore thruster does not drastically worsen the situation and, on the contrary, even seems to slightly reduce the overshoot angles for both configurations.

Compared to the zig-zag results, the turning circle appear to be less influenced by the thruster configuration. This can be seen in the top right plot of Figure 7, which compares turning circle characteristics of the 4 thrusters configuration with the 2 thrusters version with 30/70 power distribution.

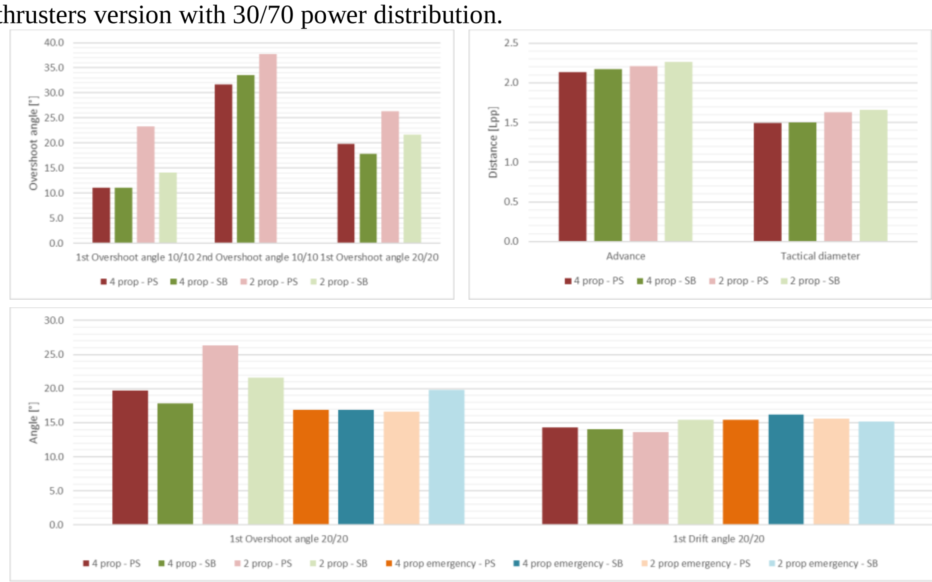


**Figure 7.** Top: overshoot angles during the zig-zags (left) and dimensions of the circle (right). Bottom: overshoot angles (left) and drift angles (right) during the emergency zig-zag 20/20, without fore propulsion.

### *3.2. Time-domain simulations*

The second phase of the manoeuvring assessment consisted in simulations to study the manoeuvrability of the 2 thruster configuration at high speed and to integrate the experiments with the results of additional manoeuvres, which could not be executed in the basin due to technical limitations. To this purpose zig-zags and turning circle simulations were conducted at full and light load draughts, both at 6 and 11 kn, focusing on the 2 thruster configurations.

MARIN software aNySIM-XMF with manoeuvring coefficient module for hull forces was used to simulate a manoeuvring ship in time domain. In order to improve accuracy and reliability of the results, the numerical model was calibrated and validated against the available experimental data.

The overshoot angles obtained from the zig-zag runs are reported as bar diagrams in Figure 8. It can be noted how, as expected, the light load has a better yaw checking behaviour with respect to the full load condition. Indeed, with lighter draught the overshoot angles decrease significantly. The influence of speed can be seen in the increase of overshoot angles at light load when switching from 6 to 11 kn. On the contrary this phenomenon is not to be seen in the full load condition. In this case, the positive effect of the increase of steering force prevails and allows to better control the vessel. The results of the turning circle simulations are also shown in Figure 8. It can be seen that the dimension of the turning circle, represented by the advance and tactical diameter, decrease when switching from full to light load.

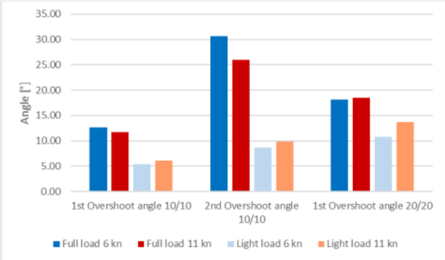

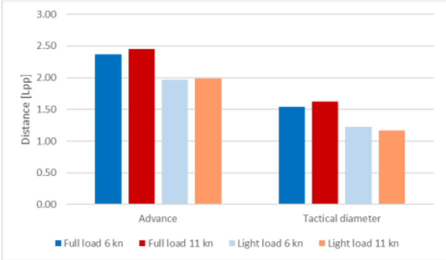


**Figure 8.** Overshoot angles from the zig-zag simulations (left) and dimensions of the circle from the 35° turning circle simulations (right), 2 thruster configuration.

## 4. Conclusions

This paper presented the hydrodynamic assessment of a double-ended ferry, with particular attention to the comparison between 2 thruster and 4 thruster configurations in addition to other special requirements.

At first a hull optimisation by means of CFD improved the bare hull resistance. This improvement was obtained by a reduction of the waterline angle at the stern and bow below the ramps, smoothening the bilges, tapering the skeg and making considerations on the nominal wake fields. These CFD results already hinted that the 2 thruster configuration is slightly better with regards the powering performance.

Successively powering model tests were performed. In addition to the two configurations, several other parameters were varied during the experiments, such as draught, geometry of the ramps and power distribution. The powering tests confirmed that the 2 thruster configuration is slightly more efficient.

Instead, from a manoeuvring point of view, free running model tests showed that the 4 thruster configuration has a slight advantage compared to the 2 thruster one, with slightly lower overshoot angles. However, when using higher steering angles, the two configurations appear to be much more similar to each other. Manoeuvring simulations complemented the manoeuvring tests by showing the influence of draught and speed on the manoeuvring characteristics.

Overall, this numerical and experimental test campaign successfully highlighted the advantages and disadvantages the both thruster configurations and provided detailed insight on the powering and manoeuvring performances.

## References

[1] Krüger S, Billerbeck H, Haack T. The propulsion and maneuvering concept of the BCF – Super C-Class double ended ferries. Proceedings of the 10th International Symposium on Practical Design of Ships and Other Floating Structures (PRADS 2007), Houston, TX, USA, 2007.

[2] Raven HC, van Hees M, Miranda S, Pensa C. A new hull form for a Venice urban transport waterbus: design, experimental and computational optimisation. Proceedings of the 7th International Symposium on Practical Design of Ships and Other Floating Structures (PRADS 1998), the Hague, the Netherlands, 1998.

[3] Vaz G, Jaouen F, Hoekstra M. Free-surface viscous flow computations; validation of URANS code FRESCO. Proceedings of the 28th ASME International Conference on Ocean, Offshore and Arctic Engineering (OMAE 2009), Honolulu, HI, USA, 2009.

[4] Grabert R. Investigation about the propulsion of double-ended ferries with two Z-drives. Proceedings of the 1st International Conference on Double Ended Ferries, Molde, Norway, 2001.